Generation of neutrino dark matter, baryon asymmetry, and radiation after quintessential inflation

Kohei Fujikura,[1,*] Soichiro Hashiba,[2,3,†] and Jun'ichi Yokoyama[2,3,4,5,‡]

[1]*Department of Physics, Kobe University, Kobe 657-8501, Japan*
[2]*Research Center for the Early Universe (RESCEU), Graduate School of Science, The University of Tokyo, Tokyo 113-0033, Japan*
[3]*Department of Physics, Graduate School of Science, The University of Tokyo, Tokyo 113-0033, Japan*
[4]*Kavli Institute for the Physics and Mathematics of the Universe (Kavli IPMU), WPI, UTIAS, The University of Tokyo, 5-1-5 Kashiwanoha, Kashiwa 277-8583, Japan*
[5]*Trans-Scale Quantum Science Institute, The University of Tokyo, Tokyo 113-0033, Japan*

(Received 26 October 2022; accepted 24 February 2023; published 24 March 2023)

We construct a model explaining dark matter, baryon asymmetry, and reheating in a quintessential inflation model. Three generations of right-handed neutrinos having hierarchical masses and the light scalar field leading to the self-interaction of active neutrinos are introduced. The lightest sterile neutrino is a dark matter candidate produced by a Dodelson-Widrow mechanism in the presence of a new light scalar field, while the heaviest and next-heaviest sterile neutrinos produced by gravitational particle production are responsible for the generation of the baryon asymmetry. Reheating is realized by spinodal instabilities of the Standard Model Higgs field induced by the nonminimal coupling to the scalar curvature, which can solve the overproduction of gravitons and curvature perturbation created by the Higgs condensation.

DOI: 10.1103/PhysRevD.107.063537

I. INTRODUCTION

It is widely believed that the very early Universe experienced exponentially accelerated expansion—so-called inflation. Inflation not only solves fundamental issues such as the horizon and flatness problems, but also provides seeds of density perturbation (see, e.g., Ref. [1] for a review of inflation). Among many possible variants of inflationary universe models, quintessential inflation [2] is interesting in the sense that the origin of dark energy is attributed to the same scalar field as the inflation-driving field dubbed the inflaton. However, this is not achieved without drawbacks, as this class of models is associated with a kination or kinetic-energy-dominant regime [3,4] after inflation without field oscillation, so that the reheating process after inflation is more involved. Note that such cosmic evolution is also realized in k-inflation [5] and a class of (generalized) G-inflation [6,7].

Traditionally, reheating in inflation models followed by a kination regime has been considered by postulating gravitational particle production [8,9] of a massless minimally coupled scalar field, which is produced with an energy density of order T_H^4 at the transition from inflation to kination [10,11]. Here $T_H = H_{\rm inf}/(2\pi)$ is the Hawking temperature of de Sitter space with the Hubble parameter $H_{\rm inf}$. In this transition, gravitons are also produced with the energy density twice as much as a massless minimally coupled scalar field, which acts as dark radiation in the later Universe. Since its energy density relative to radiation is severely constrained by observations of the cosmic microwave background (CMB) [12], we must assume creation of many massless minimally coupled fields whose energy densities dissipate in the same way as radiation throughout. Furthermore, since such a scalar field acquires a large value during inflation due to the accumulation of long-wave quantum fluctuations [13–15], particles coupled to this field tend to acquire large masses and thus thermalization is not guaranteed.

In such a situation, two of us [16] calculated the gravitational production rate of massive bosons and fermions at the transition from inflation to kination, and concluded that sufficient reheating without graviton overproduction can be achieved if they have an appropriate mass and long enough lifetime, because their relative energy density increases in time with respect to the graviton as they redshift in proportion to $a^{-3}(t)$, with $a(t)$ being the cosmic scale factor. We further applied the scenario to generations of heavy right-handed Majorana neutrinos to

*fujikura@penguin.kobe-u.ac.jp
†sou16.hashiba@resceu.s.u-tokyo.ac.jp
‡yokoyama@resceu.s.u-tokyo.ac.jp

explain the origin of radiation, baryon asymmetry, and dark matter in terms of neutrinos [17].

Unfortunately, there were two issues in the previous analysis. One is that it turned out that in order to explain the full mass spectrum of light neutrinos as inferred by neutrino oscillation, the decay rate of massive right-handed neutrinos cannot be small enough to realize appropriate reheating, as shown in Sec. III. The other issue is the role of the standard Higgs field. As discussed in Ref. [11], if it is minimally coupled to gravity, it suffers from a large quantum fluctuation during inflation [18] which will accumulate to contribute to the energy density of order $10^{-2}H_{\rm inf}^4$ at the end of inflation. Furthermore, its quantum fluctuation is so large that it acts as an unwanted curvaton, which should be removed [11].

The simplest remedy to the latter problem is to introduce a sufficiently large positive nonminimal coupling to gravity, so that it has an effective mass squared of $12\xi H_{\rm inf}^2$ during inflation, where $\xi > 0$ is the coupling constant to the Ricci scalar [19]. With this coupling, the Higgs field is confined to the origin without suffering from long-wave quantum fluctuations. Furthermore, we can automatically find another source of reheating, namely, the spinodal instability of the Higgs field, as the Ricci scalar will take a negative value in the kination regime and the Higgs field starts to deviate from the origin. Its subsequent oscillation can create particles of the Standard Model to reheat the Universe, as studied in Ref. [19].

The purpose of the present paper is to construct a consistent scenario of cosmic evolution that properly generates the observed material ingredients in the quintessential inflation model, again making use of three right-handed neutrinos with hierarchical masses inspired by the split seesaw model [20]. The heaviest and next-heaviest right-handed neutrinos realize leptogenesis and explain data from neutrino oscillation experiments via the conventional seesaw mechanism [21,22]. The nonminimally coupled Standard Model (SM) Higgs field realizes reheating after inflation via spinodal instabilities [19], while the lightest sterile neutrino and the new light scalar field lead to successful dark matter production [23].

In our scenario, baryogenesis through leptogenesis is realized by the decay of the next-heaviest right-handed neutrino with mass M_2 produced by gravitational particle production. The heaviest right-handed neutrino is assumed to be much heavier than the Hubble parameter during inflation and only provides the source of CP violation. We show the mass range of M_2 where the observed amount of baryon asymmetry is realized.

Finally, the lightest right-handed neutrino can constitute cold dark matter if it is nearly stable so that its lifetime is longer than the age of the Universe. The simplest production mechanism of such light right-handed neutrino dark matter is through neutrino oscillations between the left-handed and right-handed neutrinos, known as the Dodelson-Widrow mechanism [24], apart from gravitational particle production introducing a nonminimal coupling, as was assumed in Ref. [17]. However, constraints from x-ray observations [25–28] combined with constraints from phase-space analyses [29–31] and Lyman-α forest measurements [32–35] exclude this simplest possibility (see, e.g., Refs. [36,37] for a review of sterile neutrino dark matter).

Successful production mechanisms of right-handed neutrino dark matter have been suggested, such as resonant production [38] and production with new physics in addition to the right-handed neutrinos [39–46]. Among them, we focus on the possibility of sterile neutrino dark matter production with a secret active neutrino self-interaction originally proposed in Ref. [23]. In this scenario, a new light complex singlet scalar field that induces a self-interaction of the active neutrino is introduced. The production rate of the active neutrino in the early Universe is enhanced by the new interaction, and the resultant relic density of the lightest sterile neutrino can make up all of the dark matter in the parameter space consistent with current constraints. We calculate the relic abundance of the lightest sterile neutrino dark matter by analytically solving the Boltzmann equation under some reasonable approximations and show that a keV-scale sterile neutrino can explain the relic dark matter density when the mass scale of the new light scalar field is around an MeV.

The rest of the paper is organized as follows. In Sec. II we review the basic features of right-handed neutrinos. In Sec. III we see that a reheating of the Universe by the decay of gravitationally produced right-handed neutrino cannot be achieved, but the nonminimal coupling between the SM Higgs and the scalar curvature can lead to efficient reheating. In Sec. IV we explain baryogenesis through leptogenesis by gravitationally produced sterile neutrinos. Then, we analytically calculate the relic density produced by the lightest right-handed neutrino with a secret self-interaction of the left-handed neutrino in Sec. V. Section VI is devoted to the conclusion.

II. HIERARCHICAL STERILE NEUTRINOS

In this section, we review general features of the right-handed neutrinos. We consider the following Lagrangian density for the right-handed neutrino ν_{Ri} $(i = 1, 2, 3)$ with hierarchical masses M_i $(M_1 \ll M_2 \ll M_3)$ as in the split seesaw model [20]:

$$-\mathcal{L}_N = h_{\alpha i}\bar{L}_\alpha \tilde{H}_{\rm SM}\nu_{Ri} + \frac{1}{2}M_i\bar{\nu}_{Ri}^c\nu_{Ri} + \text{H.c.} \qquad (1)$$

In this expression, $L_\alpha = (\nu_{L\alpha}, e_{L\alpha})^{\rm T}$, $H_{\rm SM}$, and $h_{\alpha i}$ are the SM lepton doublet, SM Higgs doublet, and Yukawa coupling constants, respectively. The subscripts $\alpha = e$, μ, τ denote the generation of the SM leptons and ψ^c denotes the charge conjugation of the ψ field. After electroweak

symmetry breaking, the SM Higgs field acquires the vacuum expectation value $\langle H_{\rm SM}\rangle = v_{\rm SM}/\sqrt{2}$, where $v_{\rm SM} \simeq 246$ GeV, leading to the Dirac mass terms. The mass matrix of neutrinos is then given by

$$-\mathcal{L}_{\rm mass} = \frac{1}{2}(\bar{\nu}_L, \bar{\nu}_R^c)\mathcal{M}\begin{pmatrix}\nu_L^c \\ \nu_R\end{pmatrix} + \text{H.c.}, \quad \mathcal{M} = \begin{pmatrix}0 & m_D \\ m_D^{\rm T} & D_M\end{pmatrix}, \tag{2}$$

where $(m_D)_{\alpha i} \equiv h_{\alpha i} v_{\rm SM}/\sqrt{2}$ is the 3×3 Dirac mass matrix and $D_M \equiv \text{diag}(M_1, M_2, M_3)$. The matrix $\mathcal{M}$ can be diagonalized by the unitary matrix U:

$$U^\dagger \mathcal{M} U^* = \text{diag}(m_{\nu_{\alpha'}}, m_{N_I}), \qquad (\alpha' = 1,2,3,\ I = 1,2,3). \tag{3}$$

Assuming $m_D \ll M_i$, at leading order, the unitary matrix can be expressed as [47]

$$U = \begin{pmatrix} U_{\rm PMNS} & \theta \\ -\theta^\dagger U_{\rm PMNS} & \mathbf{1}_{3\times 3}\end{pmatrix}, \qquad \theta \equiv m_D D_M^{-1}. \tag{4}$$

In this expression, $U_{\rm PMNS}$ is the Pontecorvo-Maki-Nakagawa-Sakata (PMNS) matrix [48] defined by the following relation:

$$U_{\rm PMNS}^\dagger M_\nu U_{\rm PMNS}^* = \text{diag}(m_{\nu_1}, m_{\nu_2}, m_{\nu_3}), \qquad M_\nu \equiv -m_D D_M^{-1} m_D^{\rm T}. \tag{5}$$

For $\theta_{\alpha i} \ll 1$, the mass eigenstates $\nu_{\alpha'}$ and N_i are called active and sterile neutrinos, and are given explicitly by

$$\nu_{L\alpha} = (U_{\rm PMNS})_{\alpha\alpha'}\nu_{\alpha'} + \theta_{\alpha i} N_i^c, \qquad \nu_{Ri}^c = -\theta_{\alpha i}^* (U_{\rm PMNS})_{\alpha\alpha'}\nu_{\alpha'} + N_i^c. \tag{6}$$

One can see from the above expression that the sterile neutrino N_I almost corresponds to the right-handed neutrino ν_{Ri}. Also, the mass of the sterile neutrino N_i is almost identical to the Majorana mass of the right-handed neutrino, $m_{N_I} \simeq \delta_{Ii} M_i$ for $\theta_{\alpha i} \ll 1$, and hence we do not distinguish them in what follows.

There are several constraints on active neutrino masses from observations of neutrino oscillations such as Super-Kamiokande [49], KamLAND [50] and MINOS [51]. Absolute values of active neutrino mass-squared differences are constrained as $m_{\rm sol}^2 \equiv |m_{\nu_2}^2 - m_{\nu_1}|^2 = 7.59\times 10^{-5}$ eV^2 and $m_{\rm atm}^2 \equiv |m_{\nu_3}^2 - m_{\nu_1}^2| = 2.32\times 10^{-3}$ eV^2. One cannot take $h_{\alpha i}$ arbitrarily free since it is related to active neutrino masses through Eq. (5). To make the lightest sterile neutrino dark matter, it will turn out in Sec. V that the Yukawa coupling of the lightest sterile neutrino becomes vanishingly small, $\sum_\alpha |\tilde{h}_{\alpha 1}|^2 \ll 1$, where $\tilde{h} \equiv U_{\rm PMNS}^\dagger h$. Resultant contributions to $m_{\nu_{2,3}}$ from $\tilde{h}_{\alpha 1}$ are negligible and are decoupled in the seesaw formula. With this setup and assuming a normal mass hierarchy $m_{\nu_3} > m_{\nu_2} \gg m_{\nu_1}$, the constraints on the active neutrino masses are simplified as

$$m_{\nu_3} \simeq 0.05 \text{ eV}, \qquad m_{\nu_2} \simeq 0.01 \text{ eV}, \quad \text{and} \quad m_{\nu_1} \simeq 0. \tag{7}$$

The above condition will be used in Secs. III and IV.

III. REHEATING

In this section, we discuss reheating in our model. Before discussing the reheating mechanism in detail, we would like to clarify our setup. We consider a spatially flat Friedmann-Lemaître-Robertson-Walker background, $\mathrm{d}s^2 = -\mathrm{d}t^2 + a^2(t)\mathrm{d}\boldsymbol{x}^2$, where $a(t)$ denotes the scale factor. We consider the following smooth transition from the de Sitter phase to the kination phase [16]:

$$a^2(\eta) = \frac{1}{2}\left[\left(1 - \tanh\frac{\eta}{\Delta\eta}\right)\frac{1}{1 + H_{\rm inf}^2\eta^2} + \left(1 + \tanh\frac{\eta}{\Delta\eta}\right)(1 + H_{\rm inf}\eta)\right]. \tag{8}$$

In this expression, $H_{\rm inf}$ is the Hubble parameter during inflation, η is the conformal time which satisfies $\mathrm{d}t = a(\eta)\mathrm{d}\eta$, and $\Delta\eta > 0$ parametrizes the time scale of the transition which depends on the Lagrangian of quintessential inflation, k-inflation, or G-inflation. For $\Delta\eta \lesssim 1.7 H_{\rm inf}$, $a^2(\eta)$ is a monotonically increasing function and remains positive for all η. With this parametrization, the scale factor is normalized to unity around the end of inflation, so that $\Delta\eta$ is identical to the cosmic time scale of transition, Δt, which is identified with the physical time scale.

The energy density of gravitationally particles created during this transition has been calculated in the literature [11,16,52] as

$$\rho_\varphi = C_\varphi H_{\rm inf}^4 a^{-4}(t), \qquad (C_\varphi \simeq 5\times 10^{-3},\ \Delta t = H_{\rm inf}^{-1}) \tag{9}$$

for a massless minimally coupled scalar field φ, and

$$\rho_{\rm mf} = C_{\rm mf} m^2 H_{\rm inf}^2 e^{-4m\Delta t} a^{-3}(t), \qquad (C_{\rm mf} \simeq 2\times 10^{-3}) \tag{10}$$

for a massive fermion with mass m. In these expressions, C_φ and $C_{\rm mf}$ are numerically determined for the scale factor given by Eq. (8).

The spinodal instability of the nonminimally coupled Higgs field, on the other hand, sets in after inflation, and it takes some time until its energy starts to dissipate when its energy density behaves as [19]

$$\rho_{\rm Higgs} = C_{\rm Higgs} H_{\rm inf}^4 \frac{a^4(t_s)}{a^4(t)}. \tag{11}$$

Here $a(t_{\rm s})$ is the scale factor at the moment when the growth of spinodal instability terminates. Typically, $a^3(t_{\rm s}) \sim \mathcal{O}(10)$, but its precise value depends on ξ and Δt, where ξ is the size of the nonminimal coupling of the SM Higgs with gravity. (See the Appendix for the precise definition of ξ.) $C_{\rm Higgs}$ is sensitive to the value of ξ, which is of order $C_{\rm Higgs} \simeq 0.05 \sim \mathcal{O}(1)$ for $\xi \sim \mathcal{O}(1)$.

One can investigate the parameter region where the decay products of the sterile neutrino are the dominant source of radiation by comparing the energy density (11) with that of heavy neutrinos given by Eq. (10) at their decay time, $t_{\rm d}$. It is defined by the equality $H(t_{\rm d}) = \Gamma_{N_i}$, where $\Gamma_i = \gamma_i M_i$ with $\gamma_i \equiv \sum_\alpha |\tilde{h}_{\alpha i}|^2/(8\pi)$ [53,54] being the tree-level decay rate of N_i in the rest frame. We assume that the decay takes place during kination. In the kination-dominated era, the Hubble parameter is given by $H(t) = H_{\rm inf}/a^3(t)$, and then, the moment when the decay takes place, denoted by $t_{\rm d}$, is determined by the condition $\Gamma_i = H_{\rm inf}/a^3(t_{\rm d})$. N_i decays into SM particles that behave as radiation, and hence $\rho_{N_i}(t > t_{\rm d}) \propto a^{-4}$, where ρ_{N_i} is the energy density of N_i. By comparing the radiation energy density produced by the spinodal instability of the SM Higgs field (11) at $t = t_{\rm d}$, it turns out that the dominant component of radiation is sourced by ρ_{N_i} when

$$\frac{C_{\rm mf}}{a^4(t_{\rm s}) C_{\rm Higgs}} \left(\frac{M_i}{H_{\rm inf}}\right)^{\frac{5}{3}} e^{-4M_i \Delta t} \gamma_i^{-1/3} > 1 \tag{12}$$

is satisfied. The left-hand side of the above equation takes the maximum value when $M_i/H_{\rm inf} \simeq 0.42$ for $\Delta t = H_{\rm inf}^{-1}$. Therefore, the above condition can be expressed as

$$\gamma_i < 8.5 \times 10^{-5} \times \left(\frac{C_{\rm mf}}{a^4(t_{\rm s}) C_{\rm Higgs}}\right)^3. \tag{13}$$

As we explained in the previous section, the Yukawa coupling $\tilde{h}_{\alpha i}$ must be chosen in such a way that Eq. (7) is satisfied to explain data from neutrino oscillation experiments. This implies that there exists a nontrivial bound on γ_i. Neglecting contributions from $\tilde{h}_{\alpha 1}$, Eq. (5) can be rewritten as the following explicit expressions:

$$\begin{aligned} -\frac{v_{\rm SM}^2}{2M_2}\tilde{h}_{22}^2 - \frac{v_{\rm SM}^2}{2M_3}\tilde{h}_{23}^2 &= m_{\nu_2}, \\ -\frac{v_{\rm SM}^2}{2M_2}\tilde{h}_{32}^2 - \frac{v_{\rm SM}^2}{2M_3}\tilde{h}_{33}^2 &= m_{\nu_3}, \\ -\frac{v_{\rm SM}^2}{2M_2}\tilde{h}_{22}\tilde{h}_{32} - \frac{v_{\rm SM}^2}{2M_3}\tilde{h}_{23}\tilde{h}_{33} &= 0. \end{aligned} \tag{14}$$

The last term comes from the off-diagonal term of Eq. (5). For a normal mass hierarchy, m_{ν_α} are given by Eq. (7). Then, the magnitude of the Yukawa coupling squared is bounded as

$$\begin{aligned} \sum_\alpha |\tilde{h}_{\alpha 3}|^2 &\simeq |\tilde{h}_{23}^2| + |\tilde{h}_{33}^2| \\ &= \left| \frac{2M_3 m_{\nu_2}}{v_{\rm SM}^2} + \frac{m_{\nu_2}}{m_{\nu_3}} \tilde{h}_{33}^2 \right| + |\tilde{h}_{33}^2| \\ &\gtrsim \frac{2M_3 m_{\nu_2}}{v_{\rm SM}^2}. \end{aligned} \tag{15}$$

In the second equality we used Eq. (14). A lower bound on $\sum_\alpha |\tilde{h}_{\alpha 2}|^2$ is obtained in a similar manner. The resultant bounds are summarized as $\sum_\alpha |\tilde{h}_{\alpha i}|^2 \gtrsim 2M_i m_{\nu_2}/v_{\rm SM}^2$, for $i = 2, 3$ in the case of a normal hierarchy and, consequently, γ_i is bounded below. Using the bound on γ_i [Eq. (13)], we find that radiation is dominated by the decay of N_i when

$$M_i \lesssim 5.1 \times 10^7 \text{ GeV} \times \left(\frac{0.1}{a^4(t_{\rm s}) C_{\rm Higss}}\right)^3 \tag{16}$$

is satisfied. In the opposite region, radiation is mainly sourced by the spinodal instability of the SM Higgs field.

The above condition can be further translated into the upper bound on the reheating temperature in the case when reheating is realized by the decay products of massive neutrinos rather than spinodal instability. The time when reheating takes place, denoted by $t_{\rm RH}$, is defined by the condition $\rho_{\rm kin}(t_{\rm RH}) = \rho_{\rm rad}(t_{\rm RH})$, where $\rho_{\rm kin}$ is the kinetic energy density of the inflaton. Since $\rho_{\rm kin} \propto a^{-6}$, one can parametrize the kinetic energy of the inflaton as $\rho_{\rm kin}(t) = 3M_{\rm Pl}^2 H_{\rm inf}^2/a^6(t)$, where $M_{\rm Pl} \simeq 2.44 \times 10^{18}$ GeV is the reduced Planck mass. Then, the reheating temperature $T_{\rm RH}$ can be expressed as

$$T_{\rm RH} = \left(\frac{10}{3\pi^2 g_*(T_{\rm RH})}\right)^{\frac{1}{4}} C_{\rm mf}^{\frac{3}{4}} \gamma_i^{-\frac{1}{4}} \left(\frac{M_i}{H_{\rm inf}}\right)^{\frac{5}{4}} \frac{H_{\rm inf}^2}{M_{\rm Pl}} e^{-3M_i \Delta t} \tag{17}$$

$$\lesssim 2.2 \times 10^{-3} \frac{M_i^2}{M_{\rm Pl}} \gamma_i^{-1/4}. \tag{18}$$

Here, g_* is the number of effective degrees of freedom of the primordial hot plasma. In this calculation, we used $\Delta t = H_{\rm inf}^{-1}$, $g_*(T_{\rm RH}) = 10.75$ and $M_i/H_{\rm inf} = 0.42$, which gives the maximum reheating temperature. Again using the lower bound on γ_i given by Eq. (15), we obtain

$$T_{\rm RH} \lesssim 0.46 \text{ MeV} \times \left(\frac{0.1}{a^4(t_{\rm s}) C_{\rm Higgs}}\right)^{\frac{21}{4}}. \tag{19}$$

The above bound on the reheating temperature may be marginally consistent with the successful big bang nucleosynthesis (BBN), $T_{\rm RH} \gtrsim 0.5$ MeV [55], when

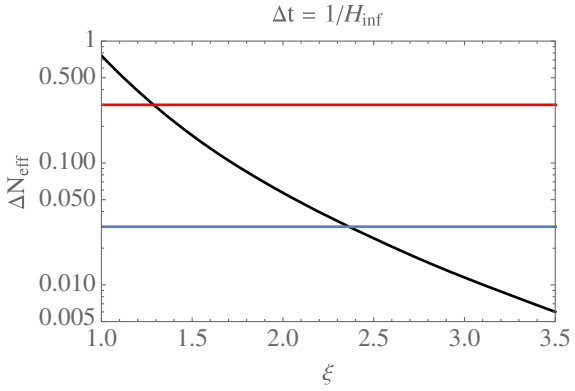

FIG. 1. Dependence of $N_{\rm eff}$ at photon decoupling on the Higgs nonminimal coupling ξ, for $\Delta t = H_{\rm inf}^{-1}$ with the quartic coupling of the SM Higgs field $\lambda_{\rm SM} = 0.01$. The red contour represents the current limit $\Delta N_{\rm eff} = 0.3$ from *Planck* data [12], while the blue contour corresponds to $\Delta N_{\rm eff} = 0.03$ which is the futuristic target sensitivity of the next-generation "Stage-4" ground-based cosmic microwave background experiment [56,57].

$a^4(t_s)C_{\rm Higgs}$ is small. Numerical calculations, however, reveal that $a^4(t_{\rm s})C_{\rm Higgs}$ is larger than 0.1 unless ξ is smaller than or very close to unity [see Fig. 1 and Eq. (24)]. Thus, for $\xi \gtrsim \mathcal{O}(1)$, the spinodal instability of the SM Higgs field should be the dominant source of radiation to realize efficient reheating, and we focus on this parameter space in the following, which corresponds to the case when the decaying sterile neutrino masses are naturally heavier than the threshold (16) and a much higher reheating temperature is realized by spinodal instability.

Before evaluating the reheating temperature in this case, let us discuss the issue of the dark radiation problem caused by gravitational particle production of gravitons. Gravitationally created gravitons are never in thermal equilibrium with SM particles, and thus they become a problematic source of dark radiation. The energy density of the total relativistic components, $\rho_{\rm tot}$, can be decomposed as the energy densities of thermal plasma consisting of the SM particles, $\rho_{\rm rad}$, and gravitons:

$$\rho_{\rm tot} = \rho_{\rm rad} + \rho_{\rm GW} = \frac{\pi^2}{30} g_*(T) T^4 + \rho_{\rm GW}. \tag{20}$$

Here, $\rho_{\rm GW}$ is the energy density of the produced gravitons. Since the graviton satisfies the same equation of motion as a massless minimally coupled scalar field, its energy density is twice that of the minimally coupled scalar field, $\rho_{\rm GW} = 2\rho_\varphi$. A constraint on dark radiation components is conventionally given in terms of the effective number of neutrino species at photon decoupling, parametrized by

$$\rho_{\rm tot}(t_{\rm ph}) = \rho_\gamma(t_{\rm ph}) \left[1 + \frac{7}{8} \left(\frac{4}{11} \right)^{\frac{4}{3}} N_{\rm eff} \right]. \tag{21}$$

In this expression, $\rho_\gamma(t_{\rm ph})$ is the energy density of photons at photon decoupling, $t = t_{\rm ph}$. Using entropy conservation, the deviation from the standard value of $N_{\rm eff}$ at photon decoupling can then be parametrized as

$$\Delta N_{\rm eff} = \frac{4}{7} \left(\frac{4}{11} \right)^{-\frac{4}{3}} g_*(t_{\rm ph}) \left(\frac{g_*(t_{\rm ph})}{g_*(t_{\rm th})} \right)^{\frac{1}{3}} \left(\frac{\rho_{\rm GW}}{\rho_{\rm rad}} \right) \Bigg|_{t=t_{\rm th}}, \tag{22}$$

where $t_{\rm th}$ is the moment when thermalization of SM fields takes place. Assuming thermalization takes place sufficiently early, $g_*(t_{\rm th}) = 106.75$ [58], and using $g_*(t_{\rm ph}) \simeq 3.38$ which is the value including the effect of nonfully decoupled neutrinos at electron-positron annihilation [59,60], Eq. (22) can be rewritten as follows:

$$\Delta N_{\rm eff} \simeq 2.36 \times \left(\frac{\rho_{\rm GW}}{\rho_{\rm rad}} \right) \Bigg|_{t=t_{\rm th}}. \tag{23}$$

The recent *Planck* data [12] give the constraint $\Delta N_{\rm eff} < 0.30$ at the 95% confidence level.

We numerically evaluate the energy density created by the spinodal instability of the SM Higgs field. The detailed numerical procedure is summarized in Ref. [19]. (See also the Appendix.) The dependence of $\Delta N_{\rm eff}$ on the nonminimal coupling ξ is shown in Fig. 1. There we use the SM Higgs quartic coupling $\lambda_{\rm SM} = 0.01$ as a reference value, although its precise value depends on the scale of $H_{\rm inf}$ and the physics around this scale because of the renormalization group effect. In the figure, we take $\Delta t = H_{\rm inf}^{-1}$, but we confirm that $\Delta N_{\rm eff}$ is less sensitive to Δt since a smaller Δt makes both the spinodal instability and graviton production large. Also, $\Delta N_{\rm eff}$ is less sensitive to a tiny quartic coupling $\lambda_{\rm SM} \lesssim 0.01$. On the other hand, from this figure one finds that $\Delta N_{\rm eff}$ is strongly sensitive to the value of ξ. This simply reflects the fact that a large ξ makes the spinodal instability large, and thus the energy density of ϕ is amplified. These results are in agreement with the earlier work in Ref. [19]. The current constraint $\Delta N_{\rm eff} < 0.3$ is compatible with $\xi \gtrsim 1.4$. Future observations by the next-generation "Stage-4" ground-based cosmic microwave background experiment will probe the parameter space $\Delta N_{\rm eff} > 0.03$ [56,57], corresponding to $\xi \lesssim 2.3$.

Since both the energy density of the Higgs field (11) and that of gravitons have only a weak dependence, from Eq. (23) we can find a one-to-one correspondence between $\Delta N_{\rm eff}$ and $C_{\rm Higgs}$ which is basically determined by ξ as

$$C_{\rm Higgs} \simeq 7.9 \times 10^{-2} \times \left(\frac{0.30}{\Delta N_{\rm eff}} \right) \times \left(\frac{1}{a^4(t_{\rm s})} \right), \quad (\Delta t = H_{\rm inf}^{-1}). \tag{24}$$

The scale factor at $t = t_{\rm RH}$ is denoted by $a_{\rm RH}$ and the reheating temperature $T_{\rm RH}$ can be evaluated as

$$a_{\rm RH} = \sqrt{\frac{3}{C_{\rm Higgs}}}\frac{M_{\rm Pl}}{H_{\rm inf}}a^{-2}(t_{\rm s}),$$
$$T_{\rm RH} = \left(\frac{10}{3}\frac{C^3_{\rm Higgs}a^{12}(t_{\rm s})}{\pi^2 g_*(T_R)}\right)^{\frac{1}{4}}\frac{H^2_{\rm inf}}{M_{\rm Pl}}. \quad (25)$$

For $H_{\rm inf} = 10^{13}$ GeV, $g_*(T_{\rm RH}) = 106.75$, and $\Delta N_{\rm eff} = 0.3$, one obtains $T_R \simeq 1.4 \times 10^6$ GeV, leading to efficient reheating compared to Eq. (19).

Before closing this section, let us estimate the thermalization temperature during kination, denoted by $T_{\rm th}$, which can be much higher than $T_{\rm RH}$ in general. Since the oscillating SM Higgs field after the growth of spinodal instabilities mainly decays into the $\mathrm{SU}(2)_{\rm W}$ gauge bosons, thermalization of SM fields is expected to take place via scattering of the SM fields mediated by the $\mathrm{SU}(2)_{\rm W}$ gauge interaction. Hence, we determine the thermalization temperature by the condition $\Gamma_{\mathrm{SU}(2)_{\rm W}}(T_{\rm th}) = H_{\rm kin}(T_{\rm th})$, where $\Gamma_{\mathrm{SU}(2)_{\rm W}}$ and $H_{\rm kin}$ are the reaction rate of scattering of SM fields through the $\mathrm{SU}(2)_{\rm W}$ gauge interaction and the Hubble parameter during kination, respectively. The reaction rate is roughly given by $\Gamma_{\mathrm{SU}(2)_{\rm W}} \sim \alpha_W^2 T$ by dimensional analysis, where $\alpha_W \equiv g_W^2/(4\pi)$ with g_W being the $\mathrm{SU}(2)_{\rm W}$ gauge coupling. $H_{\rm kin}$ can be expressed in terms of temperature in the following way. It follows from $\rho_{\rm kin} \propto a^{-6}$ and $\rho_{\rm rad}(t_{\rm RH}) = \rho_{\rm kin}(t_{\rm RH})$ that $\rho_{\rm kin}(t) = \rho_{\rm rad}(t_{\rm RH})a^6_{\rm RH}/a^6(t)$. Assuming there is no entropy generation other than the spinodal instability of the SM Higgs field, which is indeed the case in our scenario, entropy conservation leads to

$$\rho_{\rm kin}(T) = \frac{\pi^2}{30}\frac{g_*^2(T)}{g_*(T_{\rm RH})}\frac{T^6}{T^2_{\rm RH}}. \quad (26)$$

The Hubble parameter during kination is given by $H^2_{\rm kin}(T) = \rho_{\rm kin}(T)/(3M^2_{\rm Pl})$. Thus, the condition $\Gamma_{\mathrm{SU}(2)_{\rm W}}(T_{\rm th}) = H_{\rm kin}(T_{\rm th})$ yields the following relation:

$$T_{\rm th} \simeq 8.4 \times 10^{-3}\sqrt{T_{\rm RH}M_{\rm Pl}}. \quad (27)$$

Here, we put $g_W = 0.6$ and $g_*(T_{\rm th}) = g_*(T_{\rm RH}) = 106.75$. Using Eqs. (24) and (25), $T_{\rm th}$ can be further rewritten as

$$T_{\rm th} \simeq 1.6 \times 10^{-3} H_{\rm inf}\left(\frac{0.30}{\Delta N_{\rm eff}}\right)^{\frac{3}{8}}. \quad (28)$$

As is obvious from the above expression, $T_{\rm th}$ is much higher than $T_{\rm RH}$. This expression will be used in the next section.

IV. BARYOGENESIS

In this section, we discuss baryogenesis through leptogenesis in this model. We focus on the scenario where N_2 is abundantly produced by gravitational particle production and its decay is responsible for the generation of lepton asymmetry. (See, however, Ref. [61] for the possibility of thermal leptogenesis during the kination-dominated era.) The presence of N_3 provides CP violation to N_2 decay via one-loop effects. The out-of-equilibrium condition can be satisfied if $N_{2,3}$ are never in thermal equilibrium.

For $M_3 \gg H_{\rm inf} \gtrsim M_2$, the energy density of the N_3 field is exponentially suppressed and is negligible compared to that of N_2. In this parameter range, lepton asymmetry is created dominantly by the decay of N_2 with the abundance

$$n_L = \epsilon_2 \frac{\rho_{N_2}}{M_2}. \quad (29)$$

In this expression, ρ_{N_2} is the energy density of the N_2 field produced by gravitational particle production. We neglect a charged-lepton flavor effect in the calculation of the lepton asymmetry and compute the total lepton flavor asymmetry. We will justify this unflavored treatment later. ϵ_2 is the total lepton flavor asymmetry parameter, which parametrizes the CP violation of N_2 decay defined by

$$\epsilon_2 \equiv \frac{\Gamma(N_2 \to L + H_{\rm SM}) - \Gamma(N_2 \to \bar{L} + \bar{H}_{\rm SM})}{\Gamma(N_2 \to L + H_{\rm SM}) + \Gamma(N_2 \to \bar{L} + \bar{H}_{\rm SM})}. \quad (30)$$

Here, $\Gamma(X)$ is the decay rate of the reaction mode X, where final states are summed over all lepton flavors and components of the lepton and SM Higgs doublets. Nonzero ϵ_i are provided by interference between decay amplitudes of tree-level and one-loop diagrams. One-loop corrections from the vertex and self-energy [54,62,63] lead to

$$\epsilon_2 = \frac{1}{8\pi}\frac{\sum_{j\neq 2}\mathrm{Im}[\{(h^\dagger h)_{2j}\}^2]}{(h^\dagger h)_{22}}\left\{f^V\left(\frac{M_j^2}{M_2^2}\right) + f^M\left(\frac{M_j^2}{M_2^2}\right)\right\}, \quad (31)$$

where

$$f^V(x) = \sqrt{x}\left[-1 + (x+1)\ln\left(\frac{x+1}{x}\right)\right], \quad f^M(x) = \frac{\sqrt{x}}{x-1}. \quad (32)$$

For hierarchical mass $M_1/M_2 \ll M_2/M_3 < 1$, ϵ_2 is given by

$$\epsilon_2 \simeq \frac{3}{16\pi}\frac{1}{(h^\dagger h)_{22}}\mathrm{Im}\left[\{(h^\dagger h)_{23}\}^2\right]\frac{M_2}{M_3}. \quad (33)$$

Using $\mathrm{Im}(h^\dagger h)_{22} = 0$ and the definition of active neutrino mass [Eq. (5)], one can obtain an upper bound on ϵ_2 [64,65] for a normal hierarchy:

$$|\epsilon_2| \lesssim \frac{3}{8\pi}\frac{M_2 m_{\nu_3}}{v_{\rm SM}^2}. \tag{34}$$

For hierarchical active neutrino masses, ϵ_2 takes almost its maximum value unless a CP-violating phase is accidentally suppressed. We will see that this upper bound leads to bounds on M_2 in the following analysis.

The total lepton number density at the reheating temperature is estimated from Eq. (10) as

$$n_L|_{T=T_{\rm RH}} = \epsilon_2 C_{\rm mf}\left(\frac{C_{\rm Higgs}}{3}\right)^{3/2} M_2 \frac{H_{\rm inf}^5}{M_{\rm Pl}^3} a^6(t_{\rm s}) e^{-4M_2\Delta t}. \tag{35}$$

The cosmic entropy at the reheating temperature can be also calculated from Eq. (25) and is given by

$$s(T_{\rm RH}) = \frac{2}{45}\left(\frac{10}{3}\right)^{\frac{3}{4}} (\pi^2 g_*(T_{\rm RH}))^{\frac{1}{4}} C_{\rm Higgs}^{\frac{9}{4}} \frac{H_{\rm inf}^6}{M_{\rm Pl}^3} a^9(t_{\rm s}). \tag{36}$$

In this calculation, we approximate the effective number of relativistic degrees of freedom of entropy as that of the energy density. The generated lepton asymmetry is then converted into baryon asymmetry via the sphaleron process:

$$\frac{n_B}{s} = C\frac{n_L}{s}\bigg|_{T=T_{\rm RH}}. \tag{37}$$

Here, we use $C = -12/37$ corresponding to the case where the electroweak phase transition is a smooth crossover [66,67]. Then, the baryon-to-entropy ratio is expressed as

$$\begin{aligned}\left|\frac{n_B}{s}\right| &\simeq 1.3\times 10^{-3}\times\epsilon_2\left(\frac{\Delta N_{\rm eff}}{0.30}\right)^{\frac{3}{4}}\left(\frac{g_*(T_{\rm RH})}{106.75}\right)^{-\frac{1}{4}}\frac{M_2}{H_{\rm inf}}e^{-4M_2\Delta t}\\ &\lesssim 1.3\times 10^{-7}\times\left(\frac{M_2}{10^{13}\ {\rm GeV}}\right)\left(\frac{\Delta N_{\rm eff}}{0.30}\right)^{\frac{3}{4}}\left(\frac{g_*(T_{\rm RH})}{106.75}\right)^{-\frac{1}{4}}\frac{M_2}{H_{\rm inf}}e^{-4M_2\Delta t}.\end{aligned} \tag{38}$$

In the second line, we have used the inequality (34).

Since the factor $M_2/H_{\rm inf}e^{-4M_2\Delta t}$ takes the maximum value 9.2×10^{-2} for $M_2/H_{\rm inf} = 1/4$ when $\Delta t = H_{\rm inf}^{-1}$, the generated baryon asymmetry is bounded from above. The observed baryon-to-entropy ratio is given by $n_B^{\rm obs}/s \simeq 8.59\times 10^{-11}$ [12]. Thus, to produce the observed baryon asymmetry, M_2 is restricted as

$$M_2 \gtrsim 7.3\times 10^9\ {\rm GeV}\times\left(\frac{0.30}{\Delta N_{\rm eff}}\right)^{\frac{3}{4}}. \tag{39}$$

The equality is satisfied when ϵ_2 takes its maximum value and $M_2/H_{\rm inf} = 1/4$ is realized.

On the one hand, the Hubble parameter during inflation is constrained by a measurement of the tensor mode for the CMB anisotropy as $H_{\rm inf} \lesssim 4.6\times 10^{13}$ GeV [68]. The generated baryon asymmetry is thus bounded from above as

$$\begin{aligned}\left|\frac{n_B}{s}\right| &\lesssim 5.9\times 10^{-7}\times\left(\frac{\Delta N_{\rm eff}}{0.30}\right)^{\frac{3}{4}}\left(\frac{g_*(T_{\rm RH})}{106.75}\right)^{-\frac{1}{4}}\\ &\quad\times\left(\frac{M_2}{H_{\rm inf}}\right)^2 e^{-4M_2\Delta t}.\end{aligned} \tag{40}$$

The equality is satisfied when $H_{\rm inf} = 4.6\times 10^{13}$ GeV. Assuming $\Delta t = H_{\rm inf}^{-1}$ and using the observed amount of the baryon asymmetry, the above inequality can be translated into the bound on $M_2/H_{\rm inf}$ for $\Delta t = H_{\rm inf}^{-1}$. This condition turns out to be $M_2 \lesssim 1.2\times 10^{14}$ GeV for $g_*(T_{\rm RH}) = 106.75$ and $\Delta N_{\rm eff} = 0.3$. Combining with the lower bound on M_2 [Eq. (39)], we find that successful production of the observed baryon asymmetry can be realized for the following window:

$$7.3\times 10^9\ {\rm GeV}\times\left(\frac{0.30}{\Delta N_{\rm eff}}\right)^{\frac{3}{4}} \lesssim M_2 \lesssim 1.2\times 10^{14}\ {\rm GeV}. \tag{41}$$

Assuming ϵ_2 takes the maximum value (34), for $M_2 = 7.3\times 10^9$ GeV, $H_{\rm inf} = 4M_2 \simeq 2.9\times 10^{10}$ GeV, and $\Delta N_{\rm eff} = 0.30$, the observed baryon asymmetry can be achieved.

We have ignored a charged-lepton flavor effect in the calculation of the lepton asymmetry. As argued in Refs. [69–72], this calculation is oversimplified which may potentially suffer from the flavor effect when the charged-lepton Yukawa interaction is in thermal equilibrium and the reaction rate is larger than the inverse decay process, $L \to H_{\rm SM} + N_2$. This is because lepton flavor asymmetries created by the decay of N_2 lose their coherence by the charged Yukawa interaction before the inverse decay, $L \to H_{\rm SM} + N_2$. However, as noted in Refs. [72–74], this flavor effect is negligible when the inverse decay process is never in thermal equilibrium since created flavor asymmetries are not erased by the inverse decay. In our leptogenesis scenario, N_2 is nonthermally produced, and thus the unflavored calculation is justified as long as N_2 is never thermalized since the inverse decay of N_2 is kinematically forbidden.

At this benchmark point, the reheating temperature becomes $T_{\rm RH} \simeq 12$ GeV. As is obvious from Eq. (28), the out-of-equilibrium condition is maintained for this

benchmark point. In addition, the inverse decay process of N_2 is never in thermal equilibrium, and consequently the unflavored treatment in the calculation of leptogenesis is justified. We will show that N_1 makes up all dark matter at this benchmark point in the next section.

V. DARK MATTER

In this section, we discuss dark matter production in our model. We consider the scenario where the lightest sterile neutrino N_1 is a dark matter candidate, whose mass is around the keV scale. N_1 must be stable so that its signal is below the level detectable by previous and ongoing x-ray observatories, such as Chandra, XMM-Newton, Suzaku, and [75–78]. This imposes stringent constraints on the mixing angle $\sin^2 2\theta_{\alpha 1} \lesssim \mathcal{O}(10^{-14})$ for $M_1 \sim 50$ keV. For such a tiny mixing angle, contributions to active neutrino masses from $h_{\alpha 1}$ can be neglected, and thus there is no constraint on $h_{\alpha 1}$ from the neutrino oscillation experiments.

Let us consider the scenario proposed in Ref. [23] in which a self-interaction between left-handed neutrinos is introduced. The Lagrangian density is given by

$$-\mathcal{L}_\nu \supset m_\Phi^2 |\Phi|^2 + \frac{\lambda_\Phi}{2}\Phi \nu_{La}\nu_{La} + \text{H.c.} \tag{42}$$

Here, Φ is a light SM gauge-singlet complex scalar field, which possesses $B-L$ charge -2. The subscript $a = e, \mu$, or τ represents single flavors of the left-handed neutrino. An extension of multiflavor interactions is straightforward and we consider a single flavor for illustrative purposes. The above interaction is not invariant under SM gauge symmetry and is regarded as an effective interaction after electroweak symmetry breaking. Several models that produce the effective interaction (42) have been proposed [79–83]. In these models, $B-L$ is regarded as a good symmetry and we assume that $B-L$ symmetry is only violated by the Majorana mass term in Eq. (1). Under this assumption, the new interaction (42) does not wash out the generated lepton asymmetry. Although a secret self-interaction of the sterile neutrinos ($y_{ij}\nu_{Ri}^c \nu_{Rj}^c \Phi^*$) can exist, we forbid this term by imposing an approximate Z_2 symmetry $\Phi \to -\Phi$, and it has no effect on the leptogenesis discussed in the previous section.

N_1 is never in thermal equilibrium with the primordial hot plasma due to the smallness of the mixing angle and is nonthermally produced by neutrino oscillations between $\nu_{R1} \simeq N_1$ and $\nu_{L\alpha}$ as in the original model [24]. (See also the freeze-in production of the sterile neutrino proposed in Ref. [84].) In our scenario, the lepton asymmetry is of same order of magnitude as the baryon asymmetry, and hence the lepton chemical potential is negligibly small. For the light sterile neutrino mass $M_1 \ll H_{\text{inf}}$, the initial abundance of N_1 produced by gravitational particle production [Eq. (10)] is also negligible as here we do not assume the nonminimal coupling to gravity realized in Ref. [17]. Under this setup, the time evolution of the phase-space distribution function of N_1, with a fixed ratio of active neutrino energy to cosmic temperature $x \equiv E/T$, is governed by the Boltzmann equation [24,85]:

$$\frac{\mathrm{d}f_{N_1}(x,z)}{\mathrm{d}z} = \frac{\Gamma \sin^2 2\theta_{\text{eff}}}{4H(z)z} f_{\nu_{La}}(x). \tag{43}$$

In this expression, $z \equiv 1/T, \Gamma$, and $f_{\nu_{La}}(x)$ are the inverse cosmic temperature, the interaction rate, and the Fermi-Dirac distribution function for ν_{La}, respectively. $\sin^2 2\theta_{\text{eff}}$ is the effective active-sterile mixing angle including finite-temperature effects, given by

$$\sin^2 2\theta_{\text{eff}} \equiv \frac{\Delta^2 \sin^2 2\theta_{a1}}{\Delta^2 \sin^2 2\theta_{a1} + \Gamma^2/4 + (\Delta \cos 2\theta_{a1} - V^T)^2}. \tag{44}$$

Here, $\Delta \simeq M_1^2/(2E)$ and V^T is the thermal potential of ν_a. The interaction rate and thermal potential can be schematically decomposed as $\Gamma = \Gamma_{\text{SM}} + \Gamma_\Phi$ and $V^T = V^T_{\text{SM}} + V^T_\Phi$, where $\Gamma_{\text{SM}}, V^T_{\text{SM}}$ and Γ_Φ, V^T_Φ denote the SM contributions and contributions from the Φ field, respectively. The SM contributions are given by $\Gamma_{\text{SM}} \simeq G_F^2 E T^4$ [85] and $V^T_{\text{SM}} \simeq G_F E T^4/M_W^2$ [86,87], where G_F and M_W are the Fermi constant and W gauge boson mass, respectively.

We restrict ourselves to consider the parameter regime where the main production is by on-shell exchange of Φ for simplicity. (However, off-shell production can also produce the correct relic dark matter density if λ_Φ is sufficiently large [23].) Using the narrow-resonance approximation, the on-shell contribution to Γ_Φ can be estimated as [23]

$$\Gamma_\Phi = \frac{\lambda_\Phi^2 m_\Phi^2 T}{8\pi E^2}\log(1 + e^{-w/x}), \qquad w \equiv m_\Phi^2 z^2/4. \tag{45}$$

For $w/x \gtrsim 1$, the interaction rate is exponentially suppressed. Therefore, the efficient on-shell production of Φ is only possible for $m_\Phi \lesssim T$. In this parameter regime, the thermal potential from Φ is approximately given by [23]

$$V^T_\Phi = \lambda_\Phi^2 T^2/(16E). \tag{46}$$

For $\Delta > V^T, \Gamma$, the effective mixing angle can be approximated by the vacuum angle $\sin^2 2\theta_{\text{eff}} \simeq \sin^2 2\theta_{a1}$, as can be seen from Eq. (44).

When the effective mixing angle can be approximated by the vacuum angle, the Boltzmann equation (43) can be expressed by the formal integrated expression

$$\frac{f_{N_1}}{f_{\nu_{La}}} = \frac{\lambda_\Phi^2}{8\pi}\frac{M_{\rm Pl}^*}{m_\Phi}\frac{1}{x^2}\sin^2 2\theta_{a1}\int_{w_i}^{w_f} dw G(w,x),$$
$$G(w,x) \equiv w^{1/2}\log\left(1+e^{-w/x}\right). \quad (47)$$

In this calculation, we change the integration variable from z to w and use the Hubble parameter during the radiation-dominated era, $H(z) = 1/(M_{\rm Pl}^* z^2)$, with $M_{\rm Pl}^* \equiv \sqrt{90/(\pi^2 g_*(z))}M_{\rm Pl}$. w_i and w_f parametrize the integration range and $g_*(T)$ is assumed to be constant during this interval.

For $x \sim 1$, where the highest population of ν_{La} is realized, the integrand behaves as $G(w) \propto \sqrt{w}$ for $w \ll 1$ and $G(w) \propto \sqrt{w}e^{-w}$ for $w \gg 1$, and has a peak around $w \simeq 1$. This implies that N_1 is dominantly produced at $w \simeq 1$, while it is suppressed for both small and large w. Therefore, the approximations that were used to derive Eq. (47) should be justified only for $w \simeq 1$, corresponding to the temperature $T \sim m_\Phi$. Hence, the approximation $\sin^2 2\theta_{\rm eff} \simeq \sin^2 2\theta$ needs to be justified around $T \sim m_\Phi$. This requirement becomes $\Delta > V^T, \Gamma$ at $T \sim m_\Phi$, leading to the conditions $m_\Phi < M_1/\lambda_\Phi$ and $m_\Phi < \mathcal{O}(100)\ {\rm MeV}(M_1/{\rm keV})^{1/3}$. In this light-mass regime, one may approximately set the integration range as $w_i = 0$ and $w_f = \infty$ since contributions from $w \ll 1$ and $w \gg 1$ in the integrand of Eq. (47) are suppressed. Note that we slightly overestimate the relic energy density of N_1 under this approximation.

By setting $w_i = 0$ and $w_f = \infty$, f_{N_1} can be approximately calculated by integrating $g(w,x)$ in Eq. (47):

$$f_{N_1} \simeq A_1 \frac{\lambda_\Phi^2}{8\pi}\frac{M_{\rm Pl}^*}{m_\Phi}\sin^2 2\theta_{a1}\sqrt{\frac{1}{x}}f_{\nu_{La}}. \quad (48)$$

Here, $A_1 \simeq 0.769$ is the numerical constant arising from the integration of $G(w)$. It should be emphasized that the above phase-space distribution is colder than the one in the original Dodelson-Widrow mechanism, as noticed in the original paper [23]. The relic number density of N_1 can be estimated by integrating Eq. (48) and is given by

$$\frac{n_{N_1}}{n_{\nu_{La}}} = A_1\frac{A_2}{A_3}\frac{\lambda_\Phi^2}{8\pi}\frac{M_{\rm Pl}^*}{m_\Phi}\sin^2 2\theta_{a1}, \quad (49)$$

where $A_2 \simeq 1.15$, $A_3 \simeq 1.80$ are numerical constants and $n_{\nu_{La}}$ is the number density of ν_{La}. Using the number density of ν_{La} at the present time $n_{\nu_{La}} \simeq 112\ {\rm cm}^{-3}$, and the value of the critical density $\rho_0 \simeq 1.05 \times 10^{-5} h^{-2}\ {\rm GeV/cm}^3$, the relic energy density of the sterile neutrino dark matter turns out to be

$$\Omega_{N_1}h^2 \simeq 0.12 \times \left(\frac{M_1}{50\ {\rm keV}}\right) \times \left(\frac{\sin^2 2\theta_{a1}}{10^{-14}}\right) \times \left(\frac{100\ {\rm MeV}}{m_\Phi}\right) \times \left(\frac{\lambda_\Phi}{2.3\times 10^{-4}}\right)^2. \quad (50)$$

We confirm that this analytic result is in good agreement with original results for $m_\Phi < M_1/\lambda_\Phi$ where the above expression is applicable. For our parameter choice, the coupling λ_Φ is too small to be probed by laboratory experiments [79], but there exist relevant cosmological and astrophysical constraints. m_Φ must be heavier than a few MeV in order to not spoil BBN [80]. In addition, the light scalar mediator that couples to the active neutrino causes distinct changes in supernovae-collapse dynamics and imposes a stringent constraint on the light-mass regime [88–91].

For the benchmark point $M_1 \simeq 50$ keV, $\sin^2 2\theta = 10^{-14}$, $m_\Phi = 100$ MeV, and $\lambda_\Phi = 2.3 \times 10^{-4}$, the constraints mentioned above combined with x-ray observations are marginally satisfied and produce the correct dark matter relic density.

Finally, we comment on the constraint on the free-streaming length of the produced sterile neutrino dark matter and the validity of the approximations used to derive the relic dark matter density. When dark matter is produced with high velocity dispersion, it erases small-scale fluctuations and conflicts with observations such as the Lyman-α forest [35,92]. Since this constraint depends on the phase-space distribution of the produced dark matter [Eq. (48)], which is different from that in the original Dodelson-Widrow mechanism, to obtain a precise constraint we need a model-dependent analysis, which is beyond the scope of the present paper. In our analysis, we have neglected off-shell contributions. Since off-shell contributions to Γ_Φ and V_Φ^T are proportional to λ_Φ^4, an extra suppression factor λ_Φ^2 appears compared to on-shell contributions. For $\lambda_\Phi \ll 1$, the off-shell contribution is subdominant, and hence we can safely neglect this contribution. Also, using the Hubble parameter during the radiation-dominated era is justified for $T_{\rm RH} \gg m_\Phi$. This condition is satisfied for the benchmark point taken above.

VI. CONCLUSION AND DISCUSSION

In this paper, we have constructed a phenomenologically viable model that explains the production of radiation, baryon asymmetry, and dark matter within the framework of a quintessential inflation model which also accommodates dark energy by construction. Three right-handed neutrinos with hierarchical masses and a new light singlet scalar field were introduced. We have shown that the reheating achieved by the decay of the heavy sterile neutrinos leads to a reheating temperature as low as the MeV scale, contrary to Ref. [17], because of the constraint from neutrino oscillation experiments if the lightest sterile

neutrino is the dark matter candidate. In our scenario, reheating is achieved by the SM Higgs spinodal instability triggered by the nonminimal coupling of the scalar curvature. Since gravitationally produced gravitons become problematic dark radiation, the energy density of the SM Higgs field must be larger than that of gravitons to avoid the dark radiation problem, which gives a lower bound on the size of the nonminimal coupling (see Fig. 1). After the end of inflation, the next-heaviest sterile neutrino is abundantly produced by gravitational particle production and its decay is responsible for leptogenesis. The heaviest right-handed neutrino is assumed to be heavier than the Hubble parameter during inflation, and it only provides a source of CP violation for the decay of the next-heaviest sterile neutrino. To realize this scenario, the mass of the next-heaviest right-handed neutrino is restricted. The lightest right-handed neutrino with keV-scale mass is a dark matter candidate introducing a new light scalar field whose mass scale is around the MeV scale. A secret self-interaction of the active neutrino induced by the new light scalar field enhances the production rate of the lightest neutrino, and the lightest sterile neutrino can explain the correct dark matter relic density [23]. We analytically calculated the relic density of the lightest sterile neutrino under reasonable approximations for the parameter space where the production is dominated by the on-shell exchange of the new light scalar field.

Finally, we comment on the hierarchical structure of sterile neutrino masses and observable consequences of our model. In our scenario, we have assumed hierarchical Majorana masses of the right-handed neutrinos, $M_3 \gg M_2 \gg M_1$. These conditions apparently require fine-tuning, but the Randall-Sundrum model [93] can explain such huge mass hierarchies as well as the smallness of neutrino Yukawa couplings as in the split seesaw model [20]. Our model may be embedded into the split seesaw model to explain the hierarchies of sterile neutrino masses. Very interestingly, quintessential inflation can be probed by future large-scale structure surveys, as investigated in Ref. [94], while the observation of quantum-gravitational waves generated by gravitational particle production [95] may lead to a constraint on the nonminimal coupling, as discussed in Ref. [19]. (See also Ref. [96] for gravitational waves generated during quintessential inflation.)

ACKNOWLEDGMENTS

K. F. acknowledges the useful comments of Kohei Kamada and Tomohiro Nakama. We acknowledge the helpful comments of the anonymous referee. K. F. is supported by JSPS KAKENHI Grant No. JP22J00345. S. H. was supported by the Advanced Leading Graduate Course for Photon Science (ALPS). J. Y. is supported by JSPS KAKENHI Grant No. 20H05639 and Grant-in-Aid for Scientific Research on Innovative Areas 20H05248.

APPENDIX: REHEATING BY SPINODAL INSTABILITIES OF THE SM HIGGS FIELD

In this appendix, we explain the reheating scenario proposed in Ref. [19] where the energy density of the SM Higgs field from spinodal instability is a main source of cosmic entropy. The Lagrangian density of the SM Higgs field with a nonminimal coupling to the Ricci scalar is given by

$$\mathcal{L}_\phi = \sqrt{-g}\left(-\frac{1}{2}\partial_\mu\phi\partial^\mu\phi - \frac{1}{2}m^2\phi^2 - \frac{\lambda_{\rm SM}}{4}\phi^4 - \frac{1}{2}\xi R\phi^2\right). \tag{A1}$$

Here, ϕ represents the real and neutral component of the SM Higgs field. Couplings with other SM particles are omitted. The SM Higgs quartic coupling $\lambda_{\rm SM}$ is assumed to be positive up to the scale of inflation, $H_{\rm inf}$. The variational principle leads to the equation of motion for ϕ:

$$\ddot{\phi} + 3H\dot{\phi} - \frac{\nabla^2}{a^2}\phi + m^2\phi + \xi R\phi + \lambda_{\rm SM}\phi^3 = 0. \tag{A2}$$

Here, $\dot{\phi}$ is the derivative with respect to cosmic time t. Since the mass of the ϕ field is presumably much smaller than the scale of inflation and reheating when $H_{\rm inf} \gg m$, we neglect it in the following analysis.

Let us briefly explain the reheating mechanism. During inflation, $R \cong 12H_{\rm inf}^2 > 0$, and hence the nonminimal coupling becomes an effective positive mass term of ϕ field. Therefore, ϕ is initially trapped at the origin. As the kination regime commences, R becomes negative, which drives ϕ to the minimum, $\phi_M = \sqrt{-\xi R/\lambda_{\rm SM}}$. During this process, superhorizon modes of ϕ grow due to spinodal instability, and consequently the energy density of ϕ is amplified. Since the scalar curvature behaves as $R \propto a^{-6}(\eta)$ during kination, spinodal instability is soon shut off and the oscillation of ϕ takes place with the quartic potential. Finally, the oscillating ϕ field mainly decays into SM gauge bosons [97,98] and thermalization takes place. We consider the case where the growth of the ϕ field is not rapid enough to relax to ϕ_M, which is realized for $\xi \sim \mathcal{O}(1)$. (See Ref. [99] for the case $\xi \gg 1$ where ϕ soon settles down to its minimum after inflation.)

The effect of spinodal instability may be captured by the Hartree (Gaussian) approximation [100,101]. Under this approximation, one obtains $\phi^3 \simeq 3\langle\phi^2\rangle\phi$ and $\phi^4 \simeq 3\langle\phi^2\rangle^2$, where the coefficient is determined by Wick's theorem. Here, $\langle\phi^2\rangle$ is defined by

$$\begin{aligned}\langle\phi^2(\boldsymbol{x},t)\rangle &\equiv \int\frac{{\rm d}k}{k}\mathcal{P}_\phi(k,t),\\ \phi(\boldsymbol{x},t) &= \int\frac{{\rm d}^3k}{(2\pi)^{3/2}}\phi(\boldsymbol{k},t)e^{i\boldsymbol{k}\cdot\boldsymbol{x}},\\ \langle\phi(\boldsymbol{k},t)\phi^*(\boldsymbol{k}',t)\rangle &= \frac{2\pi^2}{k^3}\delta(\boldsymbol{k}-\boldsymbol{k}')\mathcal{P}_\phi(k,t).\end{aligned} \tag{A3}$$

The energy density of the SM Higgs field can be decomposed as

$$\rho_{\rm Higgs} \equiv \rho_{\rm kin} + \rho_{\rm grad} + \rho_V,$$
$$\rho_{\rm kin} = \frac{1}{2}\langle \dot{\phi}^2 \rangle, \quad \rho_{\rm grad} = \frac{1}{2}\langle (\nabla\phi)^2 \rangle, \quad \rho_V = \frac{3}{4}\lambda_{\rm SM}\langle \phi^2 \rangle^2, \tag{A4}$$

where $\rho_{\rm kin}, \rho_{\rm grad}$, and ρ_V are the kinetic energy density, gradient energy density, and potential energy density, respectively.

Introducing a rescaled field variable $\chi(\eta) \equiv a(\eta)\phi(\eta)$ and working in Fourier space, the equation of motion (A2) can be written as

$$\frac{d^2\chi_k(\eta)}{d\eta^2} + \left[k^2 + 3\lambda_{\rm SM}\langle \chi^2 \rangle + a^2(\eta)\left(\xi - \frac{1}{6}\right)R\right]\chi_k(\eta) = 0. \tag{A5}$$

Here, χ_k is the mode function of χ and $\langle \chi^2 \rangle$ is explicitly given by

$$\langle \chi^2 \rangle = \int \frac{dk}{k} P_\chi, \qquad P_\chi = \frac{k^3}{2\pi^2}|\chi_k(\eta)|^2. \tag{A6}$$

As for the boundary condition, we take the adiabatic vacuum in the remote past:

$$\chi_k(\eta) = \sqrt{\frac{1}{2k}}e^{-ik\eta}, \quad (k\eta \to -\infty). \tag{A7}$$

We numerically solve the equation of motion (A5) under the boundary condition (A7) using the fourth-order Runge-Kutta method from $H_{\rm inf}\eta = -10$. In the numerical calculation, $a(\eta)$ is approximated by Eq. (8). The mean-field value of the SM Higgs field $\langle \chi^2 \rangle$ is evaluated at each time step. Integration with respect to momentum in Eq. (A6) is UV divergent, and hence renormalization is required. χ_k with modes satisfying $k \lesssim k_M \equiv -a^2(\eta_M)(\xi - 1/6)R(\eta_M)$ experience spinodal instabilities, where η_M is the conformal time when $a^2(\eta)R$ takes its minimum negative value, and thus we simply introduce a momentum cutoff k_M to regularize the UV divergence. The energy density of the ϕ field is then evaluated using Eq. (A4).

[1] K. Sato and J. Yokoyama, Inflationary cosmology: First 30+ years, Int. J. Mod. Phys. D **24**, 1530025 (2015).
[2] P. J. E. Peebles and A. Vilenkin, Quintessential inflation, Phys. Rev. D **59**, 063505 (1999).
[3] B. Spokoiny, Deflationary universe scenario, Phys. Lett. B **315**, 40 (1993).
[4] M. Joyce, Electroweak baryogenesis and the expansion rate of the Universe, Phys. Rev. D **55**, 1875 (1997).
[5] C. Armendariz-Picon, T. Damour, and V. F. Mukhanov, k—inflation, Phys. Lett. B **458**, 209 (1999).
[6] T. Kobayashi, M. Yamaguchi, and J. Yokoyama, G-Inflation: Inflation Driven by the Galileon Field, Phys. Rev. Lett. **105**, 231302 (2010).
[7] T. Kobayashi, M. Yamaguchi, and J. Yokoyama, Generalized G-inflation: Inflation with the most general second-order field equations, Prog. Theor. Phys. **126**, 511 (2011).
[8] L. Parker, Quantized fields and particle creation in expanding universes. 1., Phys. Rev. **183**, 1057 (1969).
[9] Y. B. Zeldovich and A. A. Starobinsky, Particle production and vacuum polarization in an anisotropic gravitational field, Zh. Eksp. Teor. Fiz. **61**, 2161 (1971).
[10] L. H. Ford, Gravitational particle creation and inflation, Phys. Rev. D **35**, 2955 (1987).
[11] T. Kunimitsu and J. Yokoyama, Higgs condensation as an unwanted curvaton, Phys. Rev. D **86**, 083541 (2012).
[12] N. Aghanim *et al.* (Planck Collaboration), Planck 2018 results. VI. Cosmological parameters, Astron. Astrophys. **641**, A6 (2020).
[13] T. S. Bunch and P. C. W. Davies, Quantum field theory in de Sitter space: Renormalization by point splitting, Proc. R. Soc. A **360**, 117 (1978).
[14] A. D. Linde, Scalar field fluctuations in expanding universe and the new inflationary universe scenario, Phys. Lett. **116B**, 335 (1982).
[15] A. Vilenkin and L. H. Ford, Gravitational effects upon cosmological phase transitions, Phys. Rev. D **26**, 1231 (1982).
[16] S. Hashiba and J. Yokoyama, Gravitational reheating through conformally coupled superheavy scalar particles, J. Cosmol. Astropart. Phys. 01 (2019) 028.
[17] S. Hashiba and J. Yokoyama, Dark matter and baryon-number generation in quintessential inflation via hierarchical right-handed neutrinos, Phys. Lett. B **798**, 135024 (2019).
[18] A. A. Starobinsky and J. Yokoyama, Equilibrium state of a selfinteracting scalar field in the de Sitter background, Phys. Rev. D **50**, 6357 (1994).
[19] T. Nakama and J. Yokoyama, Reheating through the Higgs amplified by spinodal instabilities and gravitational creation of gravitons, Prog. Theor. Exp. Phys. **2019**, 033E02 (2019).
[20] A. Kusenko, F. Takahashi, and T. T. Yanagida, Dark matter from split seesaw, Phys. Lett. B **693**, 144 (2010).
[21] T. Yanagida, Horizontal gauge symmetry and masses of neutrinos, Conf. Proc. C **7902131**, 95 (1979).

[22] M. Gell-Mann, P. Ramond, and R. Slansky, Complex spinors and unified theories, Conf. Proc. C **790927**, 315 (1979).
[23] A. De Gouvêa, M. Sen, W. Tangarife, and Y. Zhang, Dodelson-Widrow Mechanism in the Presence of Self-Interacting Neutrinos, Phys. Rev. Lett. **124**, 081802 (2020).
[24] S. Dodelson and L. M. Widrow, Sterile-Neutrinos as Dark Matter, Phys. Rev. Lett. **72**, 17 (1994).
[25] A. Boyarsky, A. Neronov, O. Ruchayskiy, and M. Shaposhnikov, Constraints on sterile neutrino as a dark matter candidate from the diffuse X-ray background, Mon. Not. R. Astron. Soc. **370**, 213 (2006).
[26] A. Boyarsky, A. Neronov, O. Ruchayskiy, M. Shaposhnikov, and I. Tkachev, Where to Find a Dark Matter Sterile Neutrino?, Phys. Rev. Lett. **97**, 261302 (2006).
[27] A. Boyarsky, J. Nevalainen, and O. Ruchayskiy, Constraints on the parameters of radiatively decaying dark matter from the dark matter halo of the Milky Way and Ursa Minor, Astron. Astrophys. **471**, 51 (2007).
[28] A. Boyarsky, D. Iakubovskyi, O. Ruchayskiy, and V. Savchenko, Constraints on decaying dark matter from XMM-Newton observations of M31, Mon. Not. R. Astron. Soc. **387**, 1361 (2008).
[29] S. Tremaine and J. E. Gunn, Dynamical Role of Light Neutral Leptons in Cosmology, Phys. Rev. Lett. **42**, 407 (1979).
[30] A. Boyarsky, O. Ruchayskiy, and D. Iakubovskyi, A lower bound on the mass of dark matter particles, J. Cosmol. Astropart. Phys. 03 (2009) 005.
[31] D. Gorbunov, A. Khmelnitsky, and V. Rubakov, Constraining sterile neutrino dark matter by phase-space density observations, J. Cosmol. Astropart. Phys. 10 (2008) 041.
[32] M. Viel, J. Lesgourgues, M. G. Haehnelt, S. Matarrese, and A. Riotto, Constraining warm dark matter candidates including sterile neutrinos and light gravitinos with WMAP and the Lyman-alpha forest, Phys. Rev. D **71**, 063534 (2005).
[33] A. Boyarsky, O. Ruchayskiy, and M. Shaposhnikov, The role of sterile neutrinos in cosmology and astrophysics, Annu. Rev. Nucl. Part. Sci. **59**, 191 (2009).
[34] C. Yèche, N. Palanque-Delabrouille, J. Baur, and H. du Mas des Bourboux, Constraints on neutrino masses from Lyman-alpha forest power spectrum with BOSS and XQ-100, J. Cosmol. Astropart. Phys. 06 (2017) 047.
[35] N. Palanque-Delabrouille, C. Yèche, N. Schöneberg, J. Lesgourgues, M. Walther, S. Chabanier, and E.Armengaud, Hints, neutrino bounds and WDM constraints from SDSS DR14 Lyman-α and Planck full-survey data, J. Cosmol. Astropart. Phys. 04 (2020) 038.
[36] M. Drewes *et al.*, A white paper on keV sterile neutrino dark matter, J. Cosmol. Astropart. Phys. 01 (2017) 025.
[37] A. Boyarsky, M. Drewes, T. Lasserre, S. Mertens, and O. Ruchayskiy, Sterile neutrino dark matter, Prog. Part. Nucl. Phys. **104**, 1 (2019).
[38] X.-D. Shi and G. M. Fuller, A New Dark Matter Candidate: Nonthermal Sterile Neutrinos, Phys. Rev. Lett. **82**, 2832 (1999).
[39] M. Shaposhnikov and I. Tkachev, The νMSM, inflation, and dark matter, Phys. Lett. B **639**, 414 (2006).
[40] S. Khalil and O. Seto, Sterile neutrino dark matter in B—L extension of the standard model and galactic 511-keV line, J. Cosmol. Astropart. Phys. 10 (2008) 024.
[41] K. Kaneta, Z. Kang, and H.-S. Lee, Right-handed neutrino dark matter under the $B-L$ gauge interaction, J. High Energy Phys. 02 (2017) 031.
[42] A. Biswas and A. Gupta, Freeze-in production of sterile neutrino dark matter in $U(1)_{B-L}$ model, J. Cosmol. Astropart. Phys. 09 (2016) 044.
[43] O. Seto and T. Shimomura, Signal from sterile neutrino dark matter in extra $U(1)$ model at direct detection experiment, Phys. Lett. B **811**, 135880 (2020).
[44] V. De Romeri, D. Karamitros, O. Lebedev, and T. Toma, Neutrino dark matter and the Higgs portal: Improved freeze-in analysis, J. High Energy Phys. 10 (2020) 137.
[45] G. Bélanger, S. Khan, R. Padhan, M. Mitra, and S. Shil, Right handed neutrinos, TeV scale BSM neutral Higgs boson, and FIMP dark matter in an EFT framework, Phys. Rev. D **104**, 055047 (2021).
[46] W. Cho, K.-Y. Choi, and O. Seto, Sterile neutrino dark matter with dipole interaction, Phys. Rev. D **105**, 015016 (2022).
[47] W. Grimus and L. Lavoura, The Seesaw mechanism at arbitrary order: Disentangling the small scale from the large scale, J. High Energy Phys. 11 (2000) 042.
[48] Z. Maki, M. Nakagawa, and S. Sakata, Remarks on the unified model of elementary particles, Prog. Theor. Phys. **28**, 870 (1962).
[49] Y. Fukuda *et al.* (Super-Kamiokande Collaboration), Evidence for Oscillation of Atmospheric Neutrinos, Phys. Rev. Lett. **81**, 1562 (1998).
[50] T. Araki *et al.* (KamLAND Collaboration), Measurement of Neutrino Oscillation with KamLAND: Evidence of Spectral Distortion, Phys. Rev. Lett. **94**, 081801 (2005).
[51] P. Adamson *et al.* (MINOS Collaboration), Measurement of the Neutrino Mass Splitting and Flavor Mixing by MINOS, Phys. Rev. Lett. **106**, 181801 (2011).
[52] S. Hashiba and J. Yokoyama, Gravitational particle creation for dark matter and reheating, Phys. Rev. D **99**, 043008 (2019).
[53] M. Fukugita and T. Yanagida, Baryogenesis without grand unification, Phys. Lett. B **174**, 45 (1986).
[54] L. Covi, E. Roulet, and F. Vissani, *CP* violating decays in leptogenesis scenarios, Phys. Lett. B **384**, 169 (1996).
[55] M. Kawasaki, K. Kohri, and N. Sugiyama, Cosmological Constraints on Late Time Entropy Production, Phys. Rev. Lett. **82**, 4168 (1999).
[56] K. N. Abazajian *et al.* (CMB-S4 Collaboration), CMB-S4 science book, first edition, arXiv:1610.02743.
[57] K. Abazajian *et al.*, CMB-S4 science case, reference design, and project plan, arXiv:1907.04473.
[58] L. Husdal, On effective degrees of freedom in the early universe, Galaxies **4**, 78 (2016).
[59] G. Mangano, G. Miele, S. Pastor, T. Pinto, O. Pisanti, and P. D. Serpico, Relic neutrino decoupling including flavor oscillations, Nucl. Phys. **B729**, 221 (2005).

[60] K. Akita and M. Yamaguchi, A precision calculation of relic neutrino decoupling, J. Cosmol. Astropart. Phys. 08 (2020) 012.
[61] E. J. Chun and S. Scopel, Quintessential kination and leptogenesis, J. Cosmol. Astropart. Phys. 10 (2007) 011.
[62] M. Flanz, E. A. Paschos, and U. Sarkar, Baryogenesis from a lepton asymmetric universe, Phys. Lett. B **345**, 248 (1995).
[63] W. Buchmüller and M. Plumacher, *CP* asymmetry in Majorana neutrino decays, Phys. Lett. B **431**, 354 (1998).
[64] P. Di Bari, Seesaw geometry and leptogenesis, Nucl. Phys. **B727**, 318 (2005).
[65] O. Vives, Flavor dependence of *CP* asymmetries and thermal leptogenesis with strong right-handed neutrino mass hierarchy, Phys. Rev. D **73**, 073006 (2006).
[66] S. Yu. Khlebnikov and M. E. Shaposhnikov, The statistical theory of anomalous fermion number nonconservation, Nucl. Phys. **B308**, 885 (1988).
[67] J. A. Harvey and M. S. Turner, Cosmological baryon and lepton number in the presence of electroweak fermion number violation, Phys. Rev. D **42**, 3344 (1990).
[68] P. A. R. Ade *et al.* (BICEP/Keck Collaboration), Improved Constraints on Primordial Gravitational Waves using Planck, WMAP, and BICEP/Keck Observations through the 2018 Observing Season, Phys. Rev. Lett. **127**, 151301 (2021).
[69] E. Nardi, Y. Nir, E. Roulet, and J. Racker, The importance of flavor in leptogenesis, J. High Energy Phys. 01 (2006) 164.
[70] A. Abada, S. Davidson, F.-X. Josse-Michaux, M. Losada, and A. Riotto, Flavor issues in leptogenesis, J. Cosmol. Astropart. Phys. 04 (2006) 004.
[71] S. Blanchet and P. Di Bari, Flavor effects on leptogenesis predictions, J. Cosmol. Astropart. Phys. 03 (2007) 018.
[72] S. Blanchet, P. Di Bari, and G. G. Raffelt, Quantum Zeno effect and the impact of flavor in leptogenesis, J. Cosmol. Astropart. Phys. 03 (2007) 012.
[73] S. Blanchet and P. Di Bari, New aspects of leptogenesis bounds, Nucl. Phys. **B807**, 155 (2009).
[74] P. S. B. Dev, P. Di Bari, B. Garbrecht, S. Lavignac, P. Millington, and D. Teresi, Flavor effects in leptogenesis, Int. J. Mod. Phys. A **33**, 1842001 (2018).
[75] K. Perez, K. C. Y. Ng, J. F. Beacom, C. Hersh, S. Horiuchi, and R. Krivonos, Almost closing the νMSM sterile neutrino dark matter window with NuSTAR, Phys. Rev. D **95**, 123002 (2017).
[76] J. Kopp, Sterile neutrinos as dark matter candidates, SciPost Phys. Lect. Notes **36**, 1 (2022).
[77] K. N. Abazajian, Sterile neutrinos in cosmology, Phys. Rep. **711–712**, 1 (2017).
[78] B. M. Roach, S. Rossland, K. C. Y. Ng, K. Perez, J. F. Beacom, B. W. GrefenstetteS. HoriuchiR. KrivonosD. R. Wik, Long-exposure NuSTAR constraints on decaying dark matter in the galactic halo, Phys. Rev. D **107**, 023009 (2023).
[79] J. M. Berryman, A. De Gouvêa, K. J. Kelly, and Y. Zhang, Lepton-number-charged scalars and neutrino beamstrahlung, Phys. Rev. D **97**, 075030 (2018).
[80] N. Blinov, K. J. Kelly, G. Z. Krnjaic, and S. D. McDermott, Constraining the Self-Interacting Neutrino Interpretation of the Hubble Tension, Phys. Rev. Lett. **123**, 191102 (2019).
[81] A. de Gouvêa, P. S. B. Dev, B. Dutta, T. Ghosh, T. Han, and Y. Zhang, Leptonic scalars at the LHC, J. High Energy Phys. 07 (2020) 142.
[82] P. S. B. Dev, B. Dutta, T. Ghosh, T. Han, H. Qin, and Y. Zhang, Leptonic scalars and collider signatures in a UV-complete model, J. High Energy Phys. 03 (2022) 068.
[83] J. M. Berryman *et al.*, Neutrino self-interactions: A white paper, arXiv:2203.01955.
[84] A. Datta, R. Roshan, and A. Sil, Imprint of the Seesaw Mechanism on Feebly Interacting Dark Matter and the Baryon Asymmetry, Phys. Rev. Lett. **127**, 231801 (2021).
[85] K. Abazajian, G. M. Fuller, and M. Patel, Sterile neutrino hot, warm, and cold dark matter, Phys. Rev. D **64**, 023501 (2001).
[86] D. Notzold and G. Raffelt, Neutrino dispersion at finite temperature and density, Nucl. Phys. **B307**, 924 (1988).
[87] C. Quimbay and S. Vargas-Castrillon, Fermionic dispersion relations in the standard model at finite temperature, Nucl. Phys. **B451**, 265 (1995).
[88] G. M. Fuller, R. W. Mayle, J. R. Wilson, and D. N. Schramm, Resonant neutrino oscillations and stellar collapse, Astrophys. J. **322**, 795 (1987).
[89] G. M. Fuller, R. Mayle, and J. R. Wilson, The Majoron model and stellar collapse, Astrophys. J. **332**, 826 (1988).
[90] P.-W. Chang, I. Esteban, J. F. Beacom, T. A. Thompson, and C. M. Hirata, Towards powerful probes of neutrino self-interactions in supernovae, arXiv:2206.12426.
[91] Y.-M. Chen, M. Sen, W. Tangarife, D. Tuckler, and Y. Zhang, Core-collapse supernova constraint on the origin of sterile neutrino dark matter via neutrino self-interactions, J. Cosmol. Astropart. Phys. 11 (2022) 014.
[92] A. Dekker, S. Ando, C. A. Correa, and K. C. Y. Ng, Warm dark matter constraints using Milky-Way satellite observations and subhalo evolution modeling, Phys. Rev. D **106**, 123026 (2022).
[93] L. Randall and R. Sundrum, A Large Mass Hierarchy from a Small Extra Dimension, Phys. Rev. Lett. **83**, 3370 (1999).
[94] Y. Akrami, R. Kallosh, A. Linde, and V. Vardanyan, Dark energy, α-attractors, and large-scale structure surveys, J. Cosmol. Astropart. Phys. 06 (2018) 041.
[95] H. Tashiro, T. Chiba, and M. Sasaki, Reheating after quintessential inflation and gravitational waves, Classical Quantum Gravity **21**, 1761 (2004).
[96] M. Giovannini, Production and detection of relic gravitons in quintessential inflationary models, Phys. Rev. D **60**, 123511 (1999).
[97] D. G. Figueroa, J. Garcia-Bellido, and F. Torrenti, Decay of the standard model Higgs field after inflation, Phys. Rev. D **92**, 083511 (2015).

[98] K. Enqvist, S. Nurmi, S. Rusak, and D. Weir, Lattice calculation of the decay of primordial Higgs condensate, J. Cosmol. Astropart. Phys. 02 (2016) 057.

[99] K. Dimopoulos and T. Markkanen, Non-minimal gravitational reheating during kination, J. Cosmol. Astropart. Phys. 06 (2018) 021.

[100] D. Cormier and R. Holman, Spinodal decomposition and inflation: Dynamics and metric perturbations, Phys. Rev. D **62**, 023520 (2000).

[101] A. Albrecht, R. Holman, and B. J. Richard, Spinodal Instabilities and Super-Planckian Excursions in Natural Inflation, Phys. Rev. Lett. **114**, 171301 (2015).